A STUDY OF WAVES IN THE EARTH'S BOW SHOCK

Robert E. Holzer, Theodore G. Northrop[1], John V. Olson[2], and Christopher T. Russell
(Institute of Geophysics and Planetary Physics, University of California, Los Angeles)

1 On leave from Goddard Space Flight Center, Greenbelt, Maryland
2 Present Address: Institute of Earth and Planetary Physics, University of Alberta, Edmonton 7, Canada

Publication No. 949
University of California
Institute of Geophysics and Planetary Physics
Los Angeles

November, 1971

ABSTRACT

The perturbation vectors of waves up and downstream from the region of maximum compression in the bow shock were examined on OGO-5 under particularly steady solar wind conditions. The polarization of the upstream waves was RH, circular and of the downstream waves LH, elliptical in the spacecraft frame. By observing that the polarization of the waves remained unchanged as the shock motion swept the wave structure back and forth across the satellite three times in eight minutes, it was found that the waves were not stationary in the shock frame. A study of the methods of determining the shock normal indicates that the normal estimated from a shock model should be superior to one based upon magnetic coplanarity. The propagation vectors of the waves examined did not coincide with the shock model normal, the average magnetic field, or the plasma flow velocity. However, the major axis of the polarization ellipse of the downstream wave was nearly parallel to the upstream propagation vector.

I. INTRODUCTION

The earth's bow shock is a complex, nearly stationary wave pattern in the earth's reference frame. Details of the wave pattern differ significantly from one crossing to another. In many cases the spacecraft observes a clean transition, with a rapid rise of the magnetic field in the order of one to a few seconds as one proceeds from the interplanetary medium to the magnetosheath, while in other cases the transition extends over a minute or more and lacks the regularity observed in the first type (cf. Greenstadt et al., 1970, and references therein). In the present study, we shall be concerned only with the first type of shock transition. A prominent feature of this type of shock is that nearly monochromatic waves are superposed on the ambient field and are commonly observed both up and downstream from the region of rapid compression of the magnetic field. The precursor waves have amplitudes of the order of one gamma and lie in the frequency range from about 1 to 5 Hz, while the downstream waves have lower frequencies of the order of 0.3 Hz, and amplitudes of several gammas.

In this study, an attempt is made to determine which features are stationary in the shock frame. If, for example, it were possible to demonstrate that a wave such as the precursor is stationary in the shock frame, it would be highly useful in extending studies

of shock motion beyond the observation of the intervals between shock crossings, and permit the examination of higher frequency motions of the shock.

Waves that are stationary in the shock frame up and downstream from the shock are predicted by laminar shock theories (Sagdeev, 1962; Karpman, 1964; Crevier and Tidman, 1970). The predicted wavelengths are comparable with the thickness of the shock front. However, these laminar theories do not apply to turbulent, high Mach number shocks like the bow shock. For these thin shocks, the characteristics of up and downstream waves have been studied theoretically by Tidman and Northrop (1968), and by Perez and Northrop (1970), under the assumption that the shock is thin compared to the wavelength; by linearized theory waves are predicted to occur superposed on the ambient up and downstream magnetic fields. This theory says nothing about the shock structure or how the dissipation occurs, but merely connects the wave characteristics with the averaged (over a wavelength) magnetic fields. Travelling waves are also predicted to occur if the thin current sheet representing the shock is taken as unsteady. As will be described below, the nearly monochromatic waves that have been observed are not stationary. They are travelling, and may possibly be of long enough wavelength for the thin

shock model to apply. However, these waves seem not to be propagating normally to the shock and the work of Tidman, Perez, and Northrop would have to be extended.

The method used to test the stationary character of wave structures was to select an interval when the shock was close to the observing spacecraft and when oscillations of the shock surface repeatedly carried it across the spacecraft. Stationary structures (not monochromatic waves) can be identified by observing the same features in reverse order as the shock moves to and fro. The time scales of the to and fro motions may differ. In the case of nearly monochromatic stationary waves one might expect to observe changes in apparent frequency in the satellite frame with the oscillation of the shock. A criterion for a stationary transverse wave with circular or elliptical polarization is the reversal of the apparent direction of rotation of the magnetic vector in the spacecraft frame as the velocity of the shock passes through zero. These methods did not produce any examples of stationary monochromatic waves. The observed monochromatic waves were all definitely moving rapidly compared to the shock velocity.

II. EXPERIMENT DESCRIPTION

To study these waves we shall use data obtained by the UCLA fluxgate magnetometer flown on board OGO-5.

This magnetometer has been described in detail by Snare and Benjamin (1969) and Aubry et al. (1971) and only a few relevant details will be repeated here. The magnetometer makes one complete triaxial sample of the magnetic field during each main commutator cycle of the spacecraft. At the 8 kilobit per second telemetry rate, there are approximately 7 samples per second. The corresponding Nyquist frequency is 3.472 Hz for each axis and the total field. Each sensor can resolve the field to 1/8 gamma and thus can precisely follow field changes. However, the absolute accuracy is limited by spacecraft fields and sensor drifts. The basic magnetometer response is band limited by a fourth order low pass filter which has 8 db attenuation at half the Nyquist frequency, 20 db attenuation at the Nyquist frequency and 40 db at twice the Nyquist frequency and thus obeys the Nyquist sampling criterion.

We shall be discussing in this paper data obtained on the inbound segment of orbit 2 of OGO-5 when the satellite passed through the shock three times in rapid succession. The three crossings were particularly clean in the separation of upstream and downstream wave trains into high and low frequency regimes. The satellite was located at 13.91, -7.12, 9.60 R_E in geocentric solar ecliptic (GSE) coordinates. (For a description of coordinate systems see Russell, 1971.)

Before discussing the character of these wave trains, we shall consider the determination of the shock normal and the question of coplanarity across the shock front essential to predictions concerning these waves.

III. SHOCK NORMALS AND COPLANARITY

There are several ways to estimate the unit normal vector $\hat{n}$. Any choice of $\hat{n}$ should satisfy $\hat{n} \cdot (\vec{B}_1 - \vec{B}_2) = 0$, where $\vec{B}_1$ and $\vec{B}_2$ are the up and downstream average fields respectively. This condition only determines a plane in which $\hat{n}$ lies.

One method is to use a model normal $\hat{n}$. One of the simplest models to use is that of an earth centered conic section with azimuthal symmetry about the earth-sun line. Such a curve is described by the equation:

$$r = \frac{\ell}{1+\varepsilon\cos\theta}$$

where r is the radial distance to the shock, ε is the eccentricity, θ is the sun-earth-satellite angle and ℓ is the radial distance of the shock on the dawn-dusk plane. We shall call this Model A.

This model has the advantages that it is easy to fit and that it has an obvious scaling factor, ℓ.

Changing ℓ changes the size of the shock everywhere by the same fraction. For a given radial direction, the normal to the family of such surfaces with constant ε is independent of ℓ, the angle between the normal and the radial direction being given by:

$$\alpha = \tan^{-1}\left[\frac{\varepsilon \sin\theta}{1+\varepsilon\cos\theta}\right]$$

The disadvantages of this model are that it is earth-centered while the shock is not necessarily earth-centered and that a change in the shock position may involve a change in the eccentricity as well as the scale size.

Using OGO-1 observations of the shock front, and least square fitting these positions to the above model we obtain $\varepsilon = 0.7$ and $\ell = 23.5$ for the OGO-1 data. For the three crossings studied here, $\ell = 28.1$ and ε is retained as 0.7.

A second model has been introduced by Fairfield (1971). This model again assumes azimuthal symmetry. It is described by an equation of the form:

$$Y^2 + AXY + BX^2 + CY + DX + E = 0$$

This curve is not earth-centered but on the other hand it does not have an obvious scaling parameter. Thus, to determine a normal from this model, we have extrapolated observed shock locations along the radius

vector to this average shock position and calculated the normal to the average shock there. We shall call this Model B.

A second method is to use magnetic field coplanarity (see for example Colburn and Sonett, 1966). Magnetic coplanarity means that $\vec{B}_1$, $\vec{B}_2$ and $\hat{n}$ are coplanar:

$$\hat{n}_c = \frac{(\vec{B}_1 x \vec{B}_2) x (\vec{B}_2 - \vec{B}_1)}{|(\vec{B}_1 x \vec{B}_2) x (\vec{B}_2 - \vec{B}_1)|}$$

which by its definition satisfies $\hat{n}_c \cdot (\vec{B}_1 - \vec{B}_2) = 0$. Sufficient conditions for magnetic coplanarity are that a certain moment of the distribution function f vanish up and downstream, that there be no fluctuations with time of the fields up and downstream, and that the component of electric field normal to the shock also vanish. Let the X-axis be normal to the shock and directed downstream, the Y and Z axes being in the shock plane with $\vec{B}_1$, in the X-Z plane. Choose a frame of reference such that $\vec{v}_1$ also lies in the X-Z plane (this can always be done through order v/c by a transformation to a frame moving parallel to Y). The momentum moment of the Vlasov equation then predicts (see Tidman and Krall, 1971) from its Y component that:

$$\sum_{i,e} \int d^3v m v_y v_x f - \frac{1}{4\pi}(E_y E_x + B_y B_x)$$

is the same up and downstream. If the distribution function f up and downstream has such symmetry that the

integral vanishes (as is the case for Maxwellians) then:

$$(E_y E_x + B_y B_x)_1 = (E_y E_x + B_y B_x)_2$$

But $B_{y1} = 0$, and $E_{x1} = 0$ because $\vec{E} + \frac{\vec{v}}{c} \times B = 0$ in the absence of fluctuations. Thus:

$$B_{y2} = - \frac{(E_y E_x)_2}{B_{x2}}$$

$E_{y2} = E_{y1}$, by continuity of the tangential component of $\vec{E}$ and therefore does not vanish. If E_{x2} vanishes, so does B_{y2}, and the normal is then given by the expression for $\hat{n}_c$. If magnetic coplanarity exists, then $\vec{v}_2$ is also coplanar with $\hat{n}_c$, $\vec{B}_1$, $\vec{B}_2$, and $\vec{v}_1$.

Magnetic coplanarity may exist without $\vec{v}_1$ and $\vec{v}_2$ lying in the common plane of $\hat{n}$, $\vec{B}_1$, and $\vec{B}_2$. Suppose a frame of reference existed where all five vectors were coplanar; transformation to another frame moving parallel to the shock would leave $\hat{n}$, $\vec{B}_1$, and $\vec{B}_2$ unchanged (through order v/c) but would remove $\vec{v}_1$ and $\vec{v}_2$ from the plane.

In practice there are reasons to believe that magnetic coplanarity does not hold. Electric fields normal to the shock are often inferred (Neugebauer, 1970). A high Mach number shock such as the bow shock has turbulence associated with it which may persist ballistically into the downstream region (Tidman and Krall,

1971). If turbulence, or even travelling sinusoidal waves are present, the Y component of the momentum moment given above must be changed: the fields become time averages, as does f, but in addition there are important purely fluctuation terms when the wave amplitude is comparable with average fields, as here. Moreover, $\vec{E} + \frac{\vec{v}}{c} \times \vec{B}$ does not vanish in the presence of fluctuations. Thus we have scant reason to expect magnetic coplanarity to hold, although logically it could because the conditions spelled out above are only sufficient.

A third method that has been used to find the normal employs velocity coplanarity (mihalov, Sonett, Wolfe, 1969). This means that $\vec{v}_1 - \vec{v}_2$ is parallel to the normal, the tangential component of velocity being unchanged by the shock. Mihalov et al. find that Pioneer 6 data given better agreement with the magnetohydrodynamic shock jump conditions using a velocity coplanarity normal than using a magnetic coplanarity normal.

Figure 1a shows a plot of five second averages of the magnetic field in solar ecliptic coordinates across three shock crossings encountered by OGO-5 on 3/9/68. The accuracy of the field determination at this time has been checked by comparison with the Ames Research Center magnetometer data on Explorer 33. It is believed that the absolute vector field is accurate to within 1/2 γ at this

time. The accuracy of the relative field, that is field differences, within the interval shown here, is limited only by the quantization window of the experiment, 1/8 γ.

Table 1 lists one minute averages of the vector field in solar ecliptic coordinates observed at OGO-5 at four times: at 0546 preceding the first shock encounter; at 0549 in the magnetosheath between crossings 1 and 2; in the solar wind again at 0552; and in the magnetosheath again at 0556 after the final shock crossing.

We shall test these data to determine whether the model normals derived from average positions of the shock front are in fact permissible estimates of instantaneous shock normals. As stated above, the normal should be perpendicular to the change in field across the shock. Table 1 lists the angle η, between the shock normal and $\Delta\vec{B}$ for the three crossings for each of the two models. The calculation for Model B is based on the third of Fairfield's three shock models, with A = 0.2164; B = - 0.0986; C = -4.26; D = 44.916 and E = -623.77. This model implicitly accounts for the abberation of the solar wind by the earth's orbital motion, and assumes cylindrical symmetry about the solar direction. We have used this symmetry in deriving the shock normal at a position out of the ecliptic plane.

Model A has been used to calculate the shock normal in two ways: first, assuming the shock to be a surface

of revolution about the solar direction, and second, assuming the shock to be a surface of revolution about the flow direction using an aberration angle of 4^{o}. The angle η for the first case is listed under Model A and for the second case under Model A'.

The model normals are nearly perpendicular to the observed $\Delta\vec{B}$. Model B, however, appears to be a slightly better predictor than Model A in this case, and should be much better than Model A on the distant flanks of the shock since the Model B surface is a hyperboloid and the Model A surface, an ellipsoid. On the other hand, the calculation of the shock normal from Model A is far simpler than for Model B and yields satisfactory results when the sun-earth-probe angle is less than 60^{o}.

The coplanarity normal has also been calculated. The angle ζ between it and the model normals is given in Table I. Geometrically it is easy to see that ζ should be $\geq 90^{o}-\eta$. This is indeed the case.

IV. WAVE ANALYSIS

In this section we shall examine the character of the dominant wave trains encountered near the shock crossings shown in Figure 1a. High time resolution plots showing the three shock crossings and a section of the magnetosheath between crossings 1 and 2 are shown in Figures 1b, c, and d. The hourly average proton density and solar wind velocity were 5.1 protons cm^{-3} and 356 km/sec as measured by the Explorer 33 solar wind probe (J. Binsack, personal communication). During this interval the solar wind velocity was slowly decreasing and the density increasing from 440 km/sec and 2 protons cm^{-3} on 3/7/68 to 350 km/sec and 5 protons cm^{-3} on 3/10/68.

TABLE 1

TIME	$\vec{B}_{GSE}$			SHOCK LOCATION	η			ζ	
	X	Y	Z		MODEL A	MODEL A'	MODEL B	MODEL A	MODEL B
0546	-0.12	- 4.85	2.69	SW	84.8^{o}	86.4^{o}	90.2^{o}	18.3^{o}	15.4^{o}
0549	-5.66	-16.50	5.79	MS					
0552	0.28	- 3.97	2.85	SW	84.3^{o}	85.9^{o}	89.6^{o}	26.2^{o}	23.4^{o}
0556	-4.7-	-14.29	7.13	MS	86.6^{o}	88.2^{o}	92.5^{o}	14.8^{o}	12.6^{o}

The Mach numbers associated with these shocks were by no means unusual. The Alfven Mach number, M_A, was 7.5, and the sonic Mach number, M_s (using the measured proton temperature on Explorer 33 of 7.85×10^4 ^oK and assuming $\gamma = 5/3$ and $Te = 2Tp$), was 6.2. Measured in terms of the flow velocity parallel to the normal of Model B, M_A was 6.4 and M_s was 5.4. Furthermore, the interplanetary field was at a large angle to the estimated shock normal. Using Model B this angle was 64^o for the first shock crossing and 58^o for the last two crossings. The upstream magnetic field was nearly perpendicular to the solar wind flow and was inclined about 30^o to the ecliptic. Thus, the situation does not resemble that of a simple spiral field from the sun.

The spacecraft encountered the shock first at 0547:30 on 3/9/68, then twice more within 8 minutes, entering the magnetosheath to stay at 0554:20. The first and third crossings show rather clean separation of frequency up and downstream. In the spacecraft coordinate system B_x and B_z in the third crossing show an extremely sharp onset of the low frequency upon passing into the magnetosheath. Because the onset was not so abrupt along the Y spacecraft axis, the onsets seen in Figure 1d, which is in solar ecliptic coordinates, are not so sudden. The gradualness in the spacecraft Y component becomes mixed into the other two upon axis rotation.

The second crossing is a good deal more ragged and may have been a crossing occurring at a somewhat smaller relative spacecraft-shock velocity. Alternatively, the difference in wave structure may be due to the fact that direction of shock motion in the second crossing is opposite to that in the other two. The wave trains which dominate the spectrum of fluctuations in each region are characteristic of over 80 percent of the 500 shock crossings scanned in the OGO-3 and OGO-5 search coil magnetometer records. Characteristic power spectra computed over segments of data for the interplanetary medium just ahead of the magnetic field compression and for the magnetosheath immediately following are shown in Figure 2. The spectra derived from the upstream data show the presence of a band of frequencies centered between 0.9 Hz and 2.5 Hz although the upper limit is uncertain due to the presence of the instrument filter. We do not expect that it ranges much beyond 3 Hz (Olson et al., 1970). The amplitudes of the set of upstream fluctuations generally increases with decreasing distance from the shock compression, with amplitudes near the compression reaching a few gammas. Spectra derived from the downstream fluctuations show a broad spectrum dominated by a single line. In the cases studied here, the center frequency of the downstream wave trains does not vary by more than 0.07 Hz from 0.27 Hz. Their amplitude

diminishes with increasing distance from the compression. A 10 to 15 gamma peak to peak amplitude near the compression is not unusual.

The data were analyzed as follows. A power spectrum was computed for data intervals in the upstream or downstream region. The center frequency and bandwidth of the dominant region in each spectrum was noted. Then, the data were band-pass filtered and the filtered waveform data were analyzed using the variance ellipsoid technique, which provides the magnitude and orientation of the wave ellipsoid principal axes. For the case of a plane electromagnetic wave, the magnetic field perturbation $\vec{b}$ is normal to the wave normal vector $\vec{k}$ and thus one expects minimal variance along the direction parallel to the propagation axis. However, this method leaves a 180^{o} ambiguity in the direction in which the wave propagates.

We chose to arbitrarily assign $\vec{k}$ the direction given by cross products between sequential vectors $\vec{b}$ (compare with method of Dungey and Southwood, 1969). For a wave which is transversely polarized, the product of sequential samples should point in a direction approximately parallel (or antiparallel) to the wave normal vector $\vec{k}$. The magnitude of the product

$$\vec{A}_i = 1/2\ \vec{b}_i \times \vec{b}_{i+1}$$

approximates the area swept out by the perturbation vector between samples.

Next the scalar product between $\vec{A}_i$ and the average background field $\vec{B}$ was computed. The sign of this quantity gives an indication of the direction which the perturbation field $\vec{b}$ rotates with time around the background field in the spacecraft frame. That is, if $\vec{A} \cdot \vec{B} > 0$, $\vec{b}$ rotates in the spacecraft frame of reference about the field in a right hand sense; and if $\vec{A} \cdot \vec{B} < 0$, it rotates about the field in a left hand sense.

The results can be stated quite succinctly. The upstream $\vec{b}$ rotated about the field in a right hand sense, the downstream waves in a left hand sense in the spacecraft frame of reference. There are no exceptions to this in these wave trains. So, although the shock and satellite are alternately approaching and receding from each other, the wave polarizations remained the same. These waves must then be propagating past the spacecraft at a speed great enough that the variations in shock-satellite motion do not affect their polarization. The waves were not phase stationary in the shock frame.

The stability of the vectors is illustrated in Figure 3 which shows the relative orientation of the average unit vectors $\hat{B}_1$ and $\hat{B}_2$ as well as $\hat{k}_1$ and $\hat{k}_2$

with respect to the shock normal. The vector $\hat{k}_1$ remained within 15^o of its indicated position during the entire time that the satellite was in the interplanetary medium within the interval shown in Figure 1a. During the same interval $\hat{k}_2$ remained within 30^o of its indicated position while the satellite was in the magnetosheath.

In Figure 4 the polarized power (see Born and Wolf, 1970) is shown as a function of time, the light graph for the total frequency band below 3.5 Hz (the Nyquist frequency) and the heavy graph for the band from 0.8 to 3.5 Hz. It may be noted that the high frequency polarized power is found upstream from the shock compression but decreases rapidly downstream from the compression. The total polarized power is dominated by the low frequency wave in the magnetosheath. The term sin 2β is a polarization parameter defined by Born and Wolf (1970). It has the values +1 when the polarization is right handed and circular, -1 when left handed and circular, and 0 when linear. It may be noted that the right hand circular polarization is consistent in the interplanetary medium near the shock. (In this discussion the sense of rotation of $\hat{b}$ is with reference to $\vec{B}$ rather than $\hat{k}$ as in optics.) There is a strong tendency for the polarization to remain left handed with a relatively low ellipticity in the magnetosheath. The ratio of the major

to minor axes remained less than 3.

The major axis of the downstream waves displayed an interesting geometrical relationship to the upstream waves. It was nearly parallel to the propagation vector of the upstream waves, as illustrated in Figure 5. This may indicate some spatial ordering with respect to the currents in the shock.

V. SUMMARY AND CONCLUSIONS

The bow shock normal, which is useful in any analysis of shock wave structure, can be derived satisfactorily in these three crossings from a bow shock model. Under quiet solar wind conditions such a model normal is very likely superior to a normal computed on the assumption of magnetic coplanarity. First, the latter suffers from the difficulty of determining the value of the ambient magnetic field with sufficient accuracy. Further, we have shown that in the presence of magnetic field fluctuations, or of an electric field normal to the shock, the shock normal, the upstream magnetic field, and the downstream magnetic field are not coplanar. Recent experimental evidence indicates that a normal electric field exists under some circumstances; also large amplitude magnetic fluctuations are clearly present here. We, therefore, discount the coplanarity normal as being of value here.

An interval of very steady solar wind conditions, during which the bow shock crossed the OGO-5 satellite three times within less than 10 minutes, was selected for detailed study. The wave trains up and downstream from the region of most rapid compression of the magnetic field were not stationary in the shock frame since they exhibited no polarization reversal as the shock motion relative to the satellite reversed. In the spacecraft frame the upstream waves were continuously right hand circularly polarized and the downstream waves, left hand elliptically polarized. While the propagation vectors of the waves did not coincide with the shock normal or with ambient magnetic fields, it was noted that the direction of the major axis of the polarization ellipse of the downstream waves, immediately downstream from the shock compression, was nearly parallel to the upstream wave propagation vector. This observation may be more than mere coincidence.

There is no intent to draw broad generalizations from the study of one carefully selected shock situation since the wave structure is undoubtedly influenced by several factors including the orientation of the magnetic field with respect to the shock normal. However, the solar wind was close to its average condition and it is probable that the results described may always be found in some parts of the bow shock under normal solar wind conditions.

VI. ACKNOWLEDGMENTS

We are indebted to the coinvestigators Paul J. Coleman, Jr., Thomas A. Farley, and Darrell L. Judge for providing us with OGO-5 fluxgate magnetometer data, and to J. Binsack for providing the Explorer 33 MIT plasma probe data. We are also indebted to Joseph D. Means for assistance in the analysis.

This report represents one aspect of research done by the Jet Propulsion Laboratory for the National Aeronautics and Space Administration under NASA contract 7-100, GSFC-623-S-70-31. Financial support for the work at the University of California was provided by the Jet Propulsion Laboratory under contract 950403 and National Aeronautics and Space Administration contract NGR-05-007-276.

REFERENCES

Aubry, M. P., M. G. Kivelson, and C. T. Russell, Motion and structure of the magnetopause, J. Geophys. Res., 76 (7), 1673, 1971.

Born, M., and E. Wolf, Principles of Optics, Fourth Edition, Pergamon Press, Oxford, 1970.

Colburn, D. S., and C. P. Sonett, Discontinuities in the solar wind, Space Science Reviews, 5, 439, 1966.

Crevier, W. F., and D. A. Tidman, Oblique shocks and finite β plasmas, Phys. Fluids, 13, 2275, 1970.

Dungey, J. W., and D. J. Southwood, Ultra low frequency waves in the magnetosphere, Space Science Reviews, 10, 672, 1970.

Fairfield, D. H., Average and unusual locations of the earth's magnetopause and bow shock, J. Geophys. Res., in press, 1971.

Greenstadt, E. W., I. M. Green, G. T. Inouye, D. S. Colburn, J. H. Binsack, and E. F. Lyon, Dual satellite observations of the earth's bow shock I: The thick pulsation shock, Cosmic Electrodynamics, 1, 160, 1970.

Karpman, V. I., Structure of the shock front propagating at an angle to a magnetic field in a low density plasma, Sov. Phys. JETP Engl. Transl., 8, 715, 1964.

Mihalov, J. D., C. P. Sonett, and J. H. Wolfe, MHD Rankine-Hugoniot equations applied to earth's bow shock, J. of Plasma Phys., 3 (3), 449, 1969.

Neugebauer, M., Initial deceleration of solar wind positive ions in the earth's bow shock, J. Geophys. Res., 75, 717, 1970.

Olson, J. V., R. E. Holzer, and E. J. Smith, High frequency fluctuations associated with the earth's bow shock, J. Geophys. Res., 74, 4601, 1969.

Perez, J. K., and T. G. Northrop, Stationary waves produced by the earth's bow shock, J. Geophys. Res., 75, 6011, 1970.

Russell, C. T., Geophysical coordinate transformations, submitted to Cosmic Electrodynamics, 1971.

Sagdeev, R. Z., The fine structure of a shock wave front propagated across a magnetic field in a rarified plasma, Sov. Phys. JETP Engl. Transl., 6, 867, 1962.

Snare, R. C., and C. R. Benjamin, Magnetic field instrument for the OGO-E spacecraft, IEEE Trans. on Nucl. Sci., NS-13, 333, 1966.

Tidman, D. A., and T. G. Northrop, Emission of plasma waves by the earth's bow shock, J. Geophys. Res., 73, 1543, 1968.

Tidman, D. A., and N. A. Krall, Shock Waves in a Collisonless Plasma, John Wiley, New York, 1971.

FIGURE CAPTIONS

Figure 1a

Three bow shock crossings on OGO-5, orbit 2, inbound. The magnetic field in gamma is a 5 second average. The coordinates are geocentric solar ecliptic.

Figure 1b, c, d

Expanded time scale (seven points per second) diagrams of the three shock crossings shown in 1a.

Figure 2

Two characteristic sets of power spectra, log power (gamma^2 Hz^{-1}) vs. log frequency (Hz). The four diagrams at the left are for the near interplanetary medium and the four at the right are for the magnetosheath just inside the region of maximum field compression. The spectral computations were for 1024 points with 20 degrees of freedom.

Figure 3

Diagram showing the orientation of several vectors with respect to the shock normal, N, chosen as the X-axis. The XZ plane was chosen to include the unit upstream B vector ($\hat{B}_1$). $\hat{B}_2$ is the unit downstream B vector; $\hat{k}_1$ and $\hat{k}_2$ are the unit up and downstream wave normals, respectively, $\hat{v}_{sw}$, the unit solar wind vector and $\hat{M}$, the unit vector of the major axis of the downstream polarization ellipse.

Figure 4

Diagram showing stability of polarization pattern. The total value of B is included to show the relation to shock crossings. The light graph in line 2 indicates total polarized power below 3.5 Hz and the heavy graph indicates polarized power between 0.8 and 3.5 Hz. In the third line sin 2β is a polarization parameter with value +1 corresponding to right handed circular polarization and -1 to left handed circular polarization.

Figure 5

Diagram showing the relation between the upstream ($\hat{k}_1$) and downstream ($\hat{k}_2$) wave normal vectors and the direction of the major axis of the downstream polarization ellipse ($\hat{M}$).

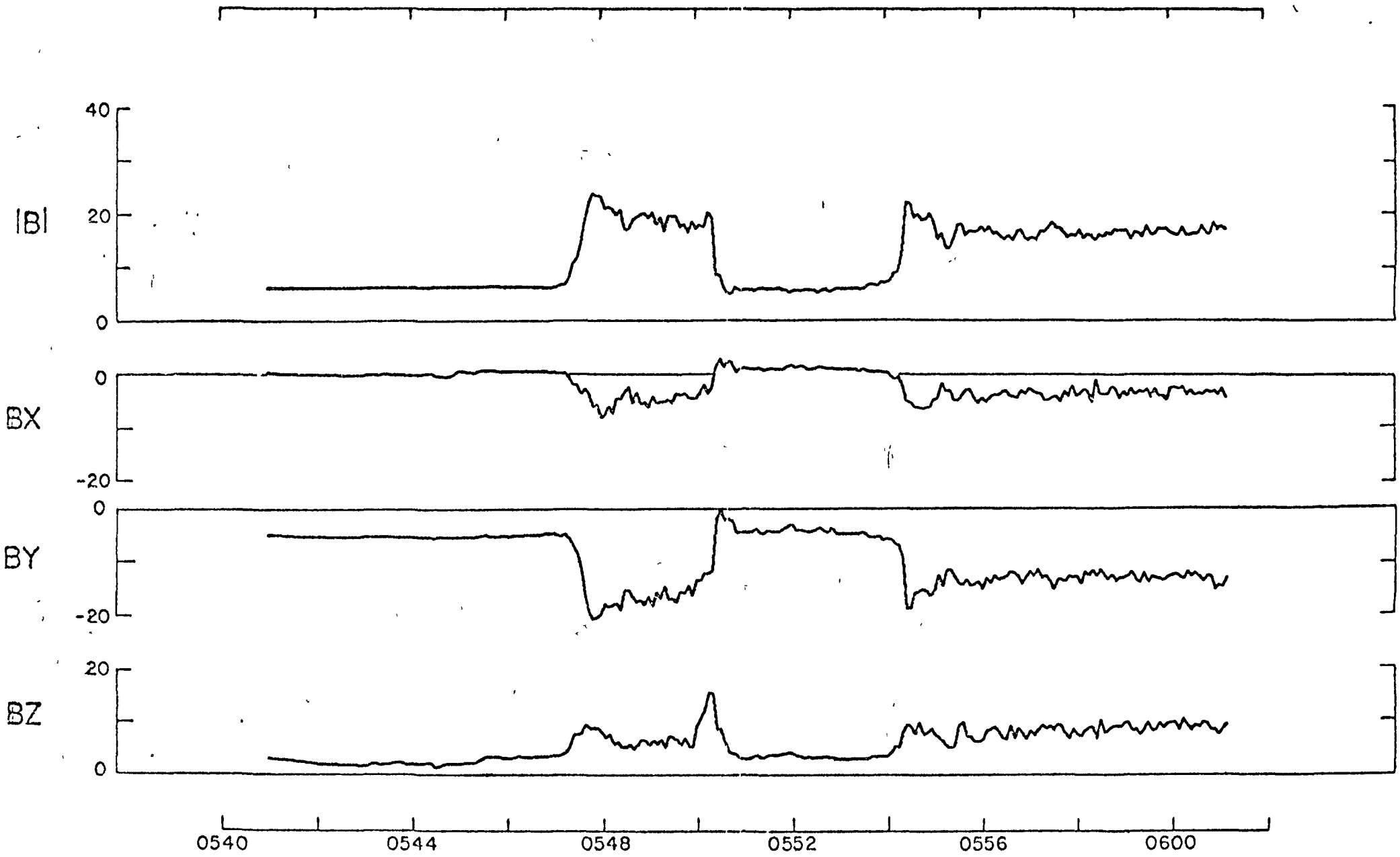
40
20
0
|B|
0
-20
BX
0
-20
BY
20
0
BZ
0540
0544
0548
0552
0556
0600
UNIVERSAL TIME
3/9/68

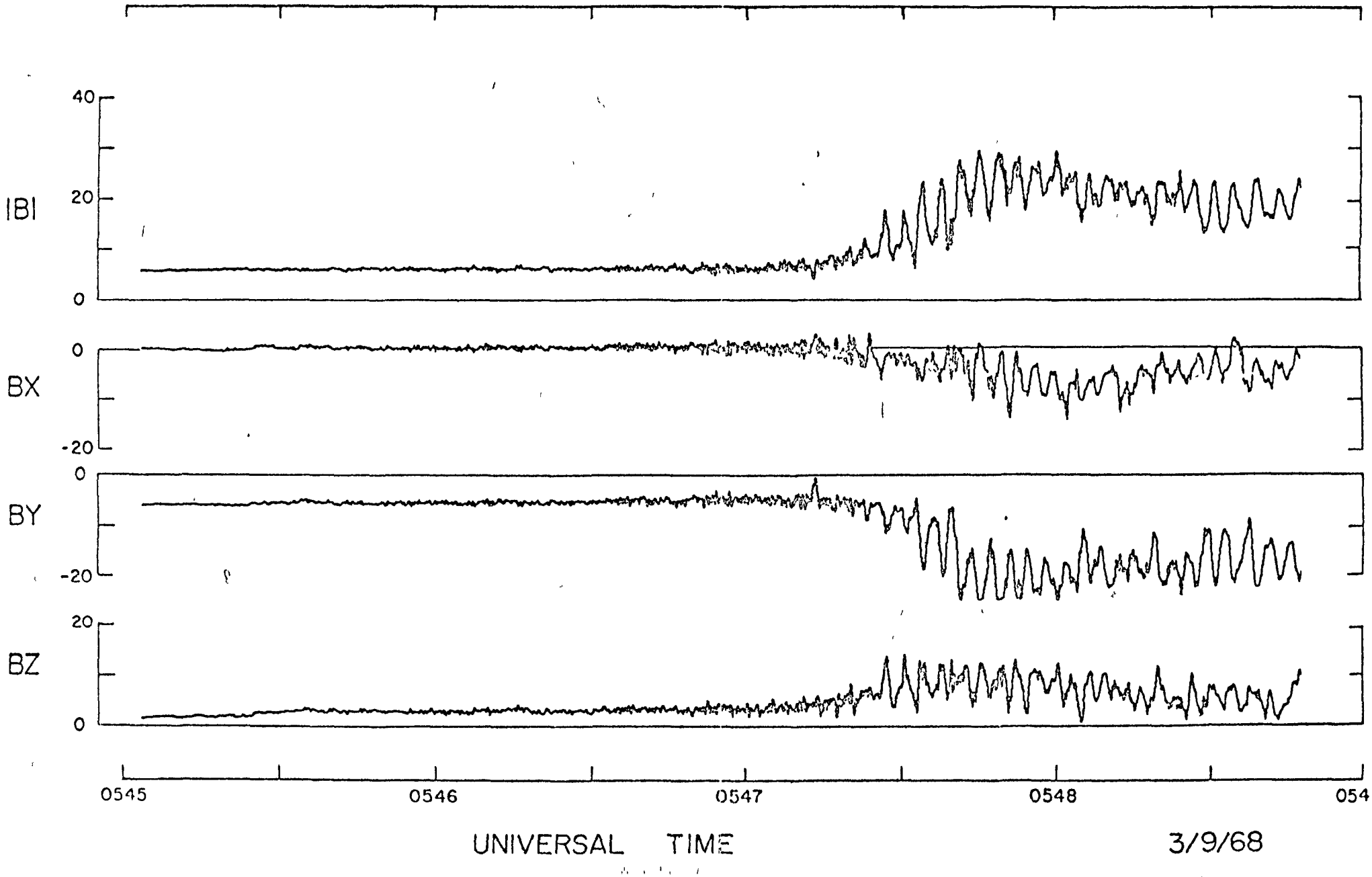
40
20
0
IBI
0
-20
BX
0
-20
BY
20
0
BZ
0545
0546
0547
0548
0549
UNIVERSAL TIME
3/9/68

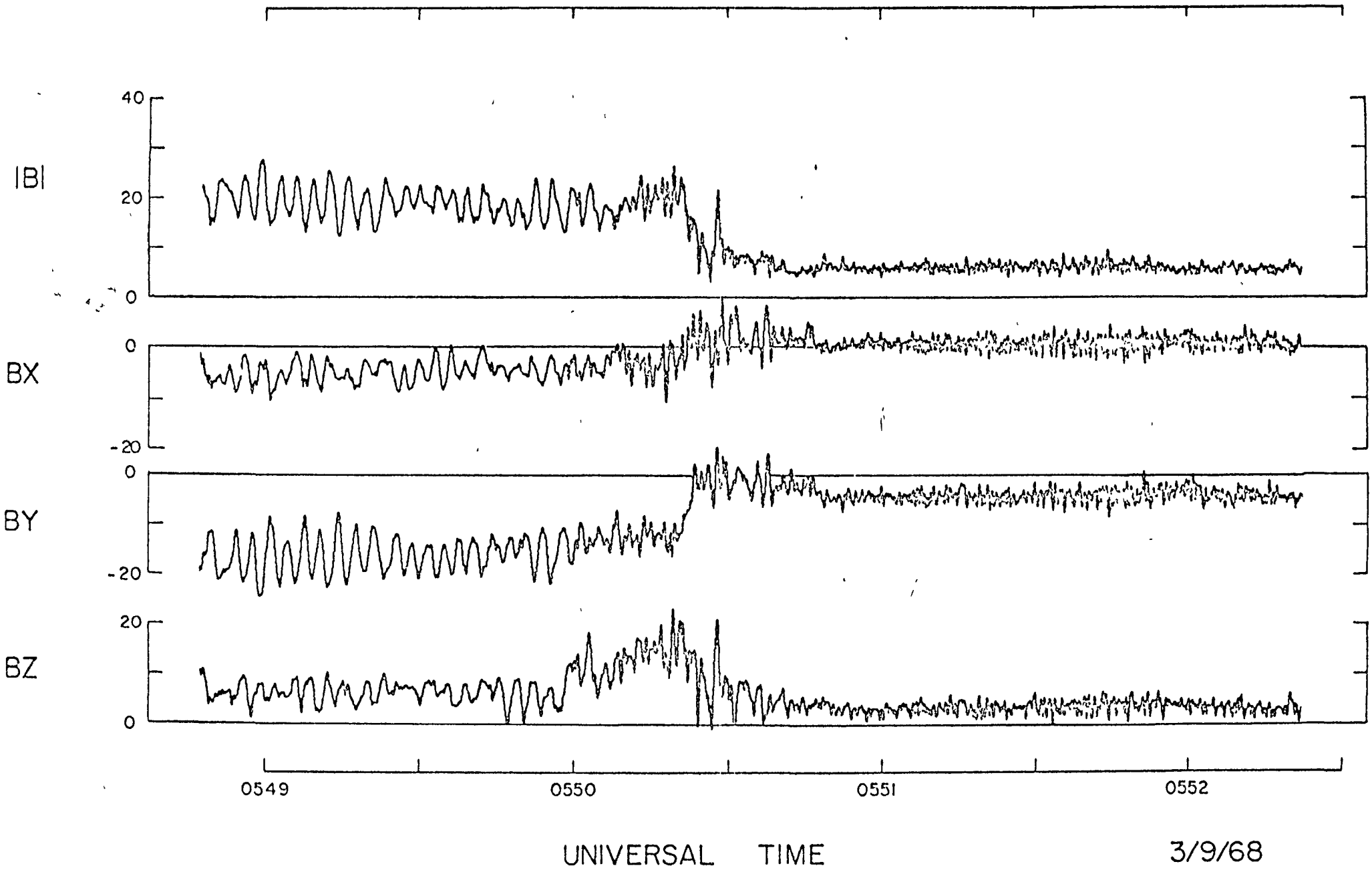
40
20
0
|B|
0
BX
-20
0
BY
-20
20
BZ
0
0549
0550
0551
0552
UNIVERSAL TIME
3/9/68

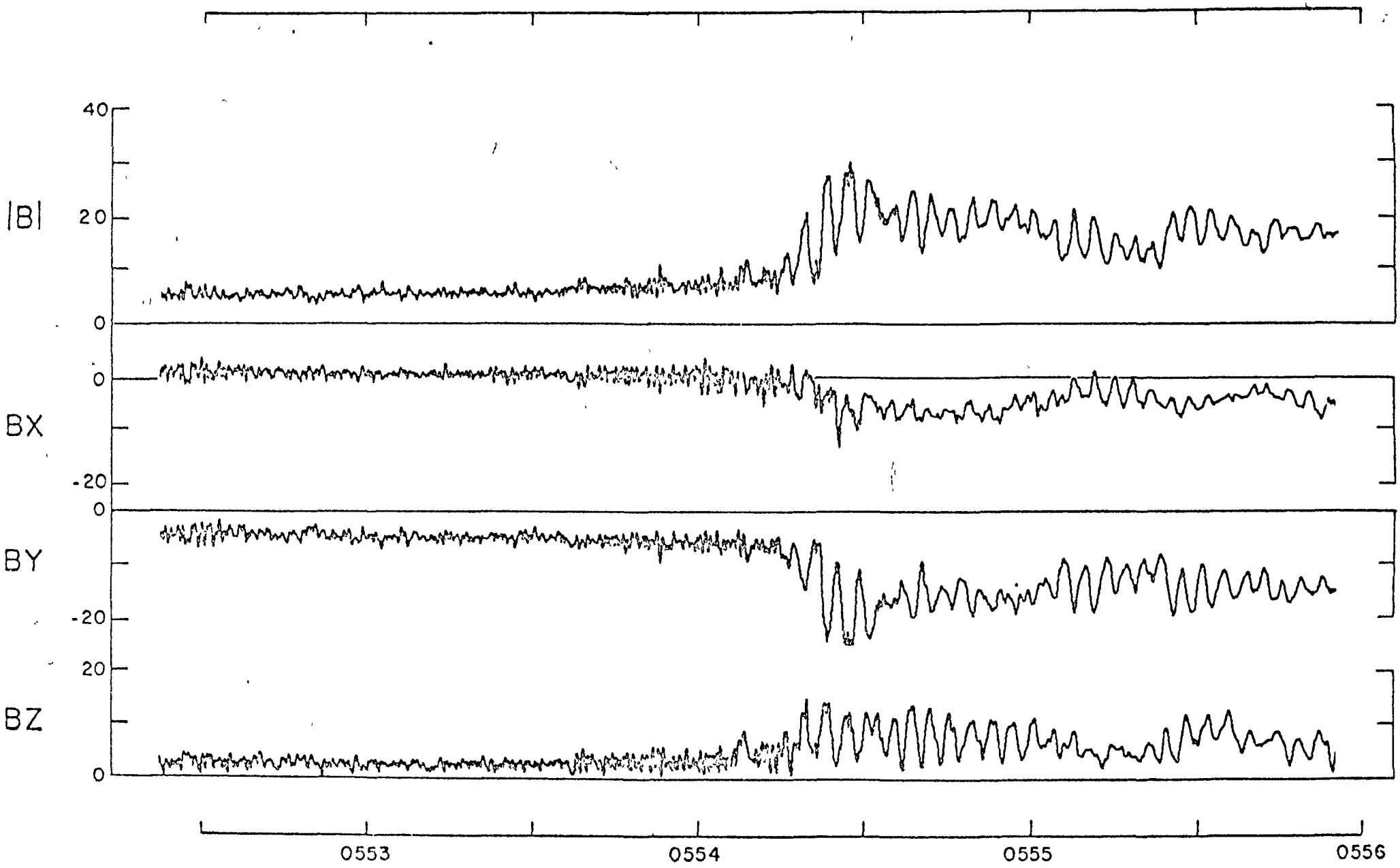
40
|B|
20
0
0
BX
-20
0
BY
-20
20
BZ
0
0553
0554
0555
0556
UNIVERSAL TIME
3/9/68

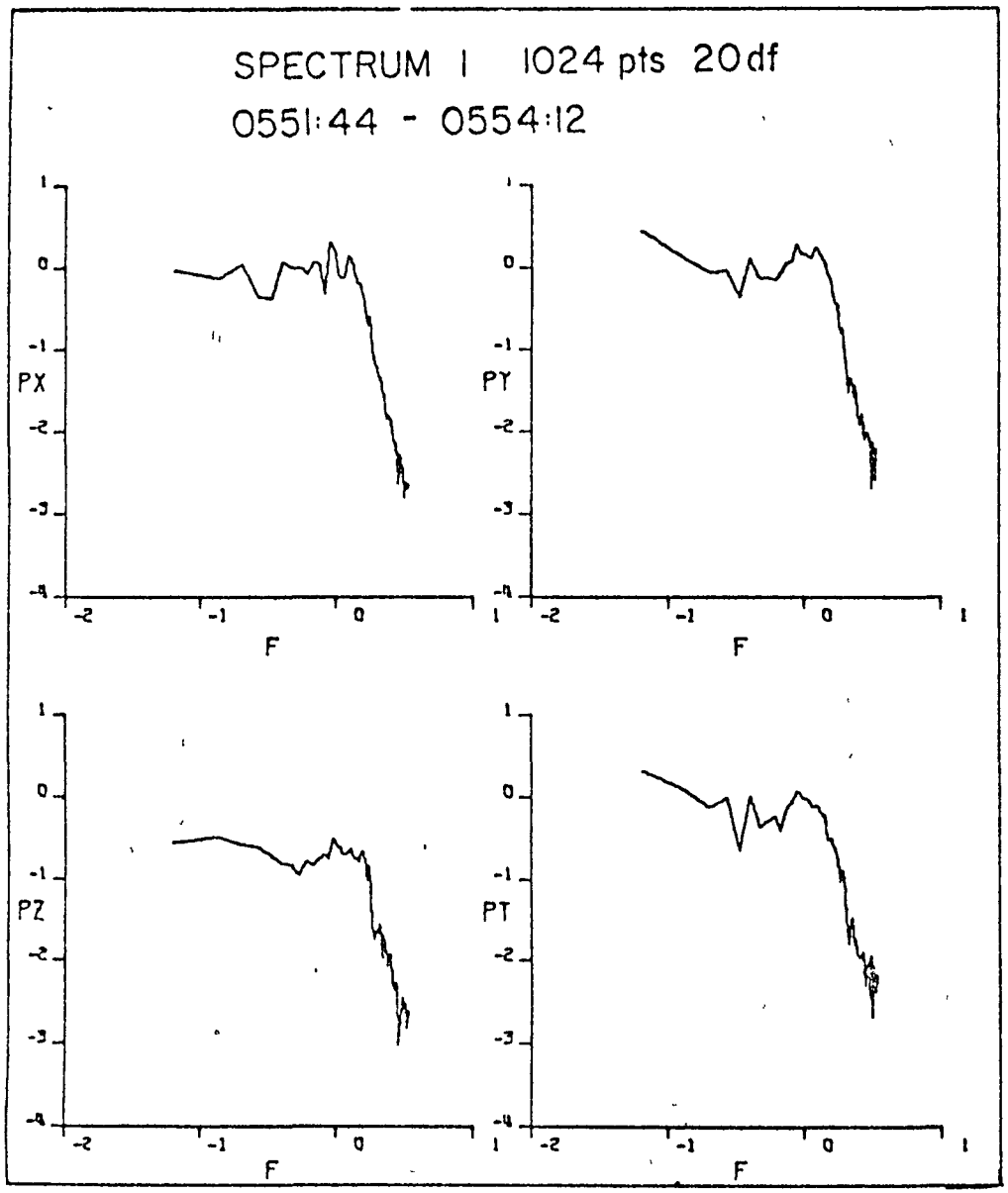
SPECTRUM 1 1024 pts 20df
0551:44 - 0554:12
PX
PY
PZ
PT
F

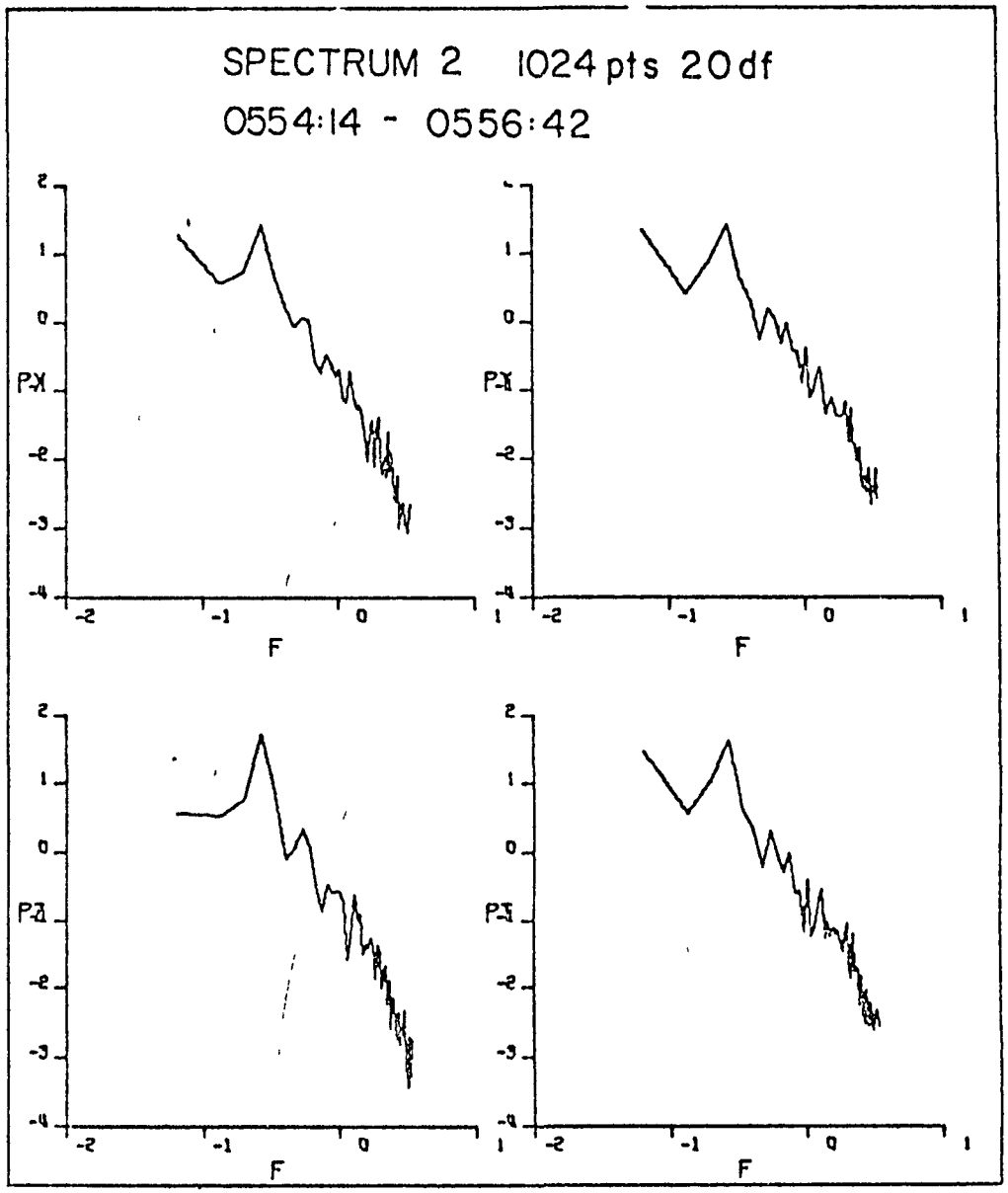
SPECTRUM 2 1024 pts 20df
0554:14 - 0556:42
F

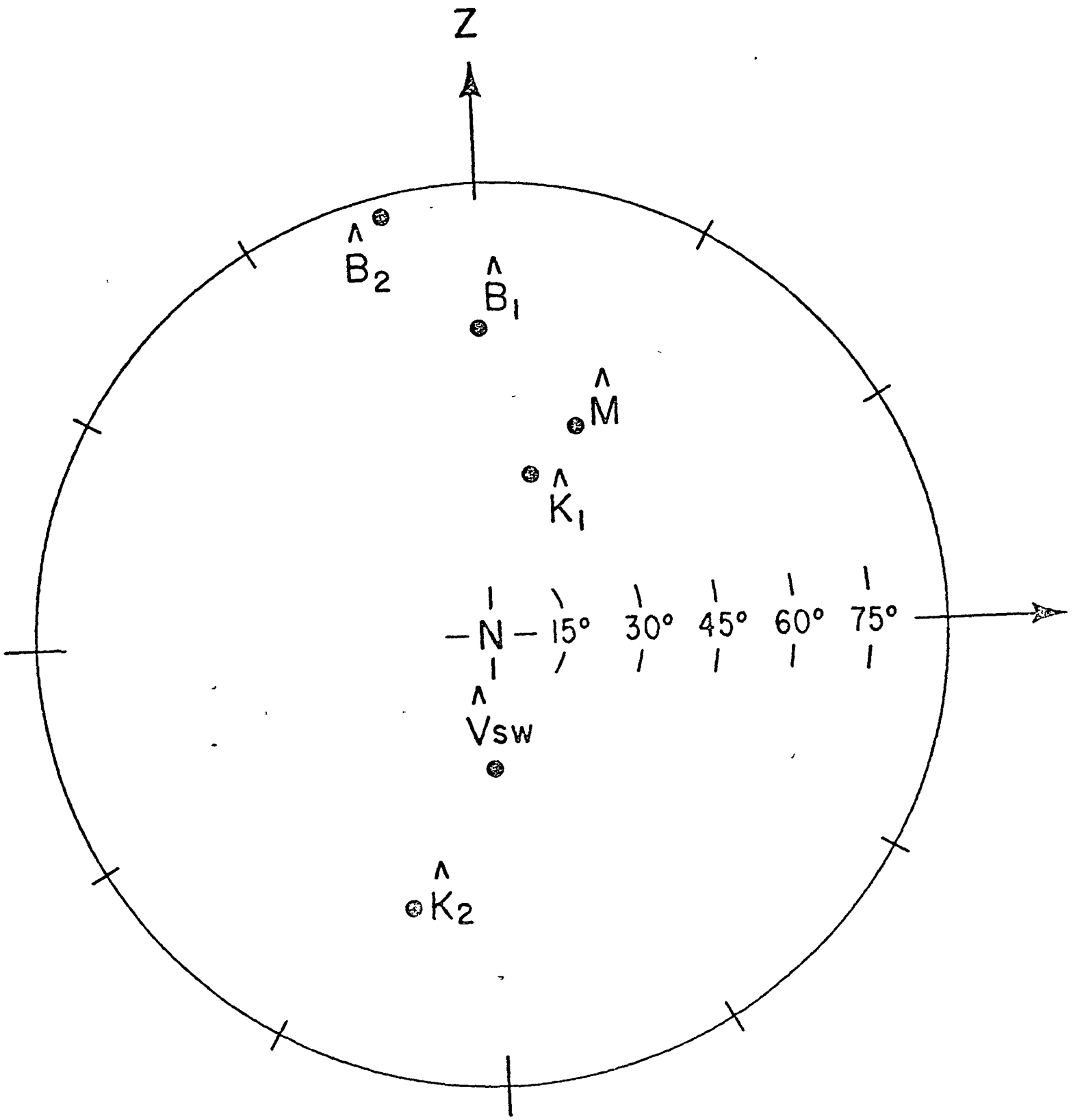
Z
B2
B1
M
K1
N
15°
30°
45°
60°
75°
Vsw
K2

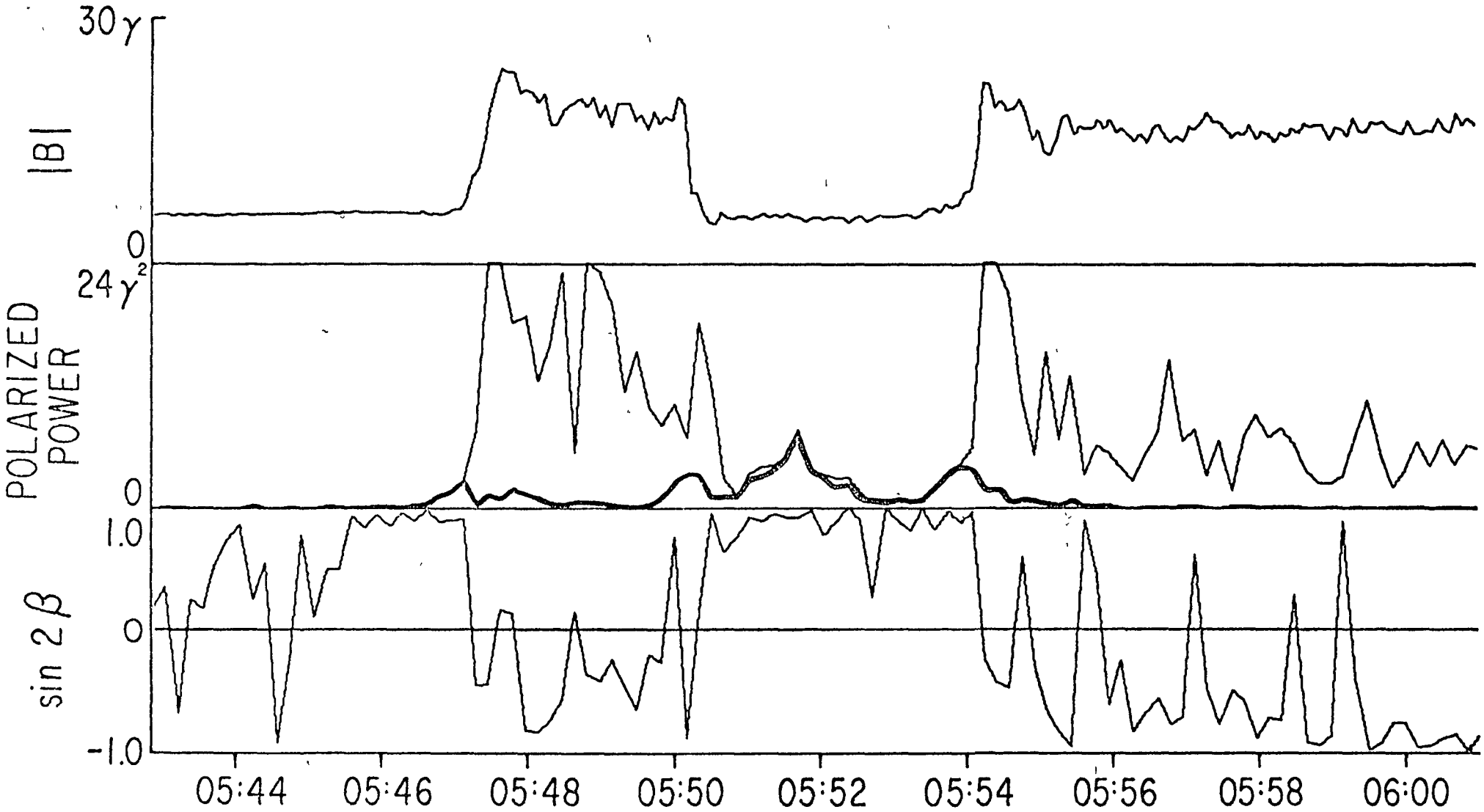
30γ
|B|
0
24γ²
POLARIZED POWER
0
1.0
sin 2β
0
-1.0
05:44
05:46
05:48
05:50
05:52
05:54
05:56
05:58
06:00

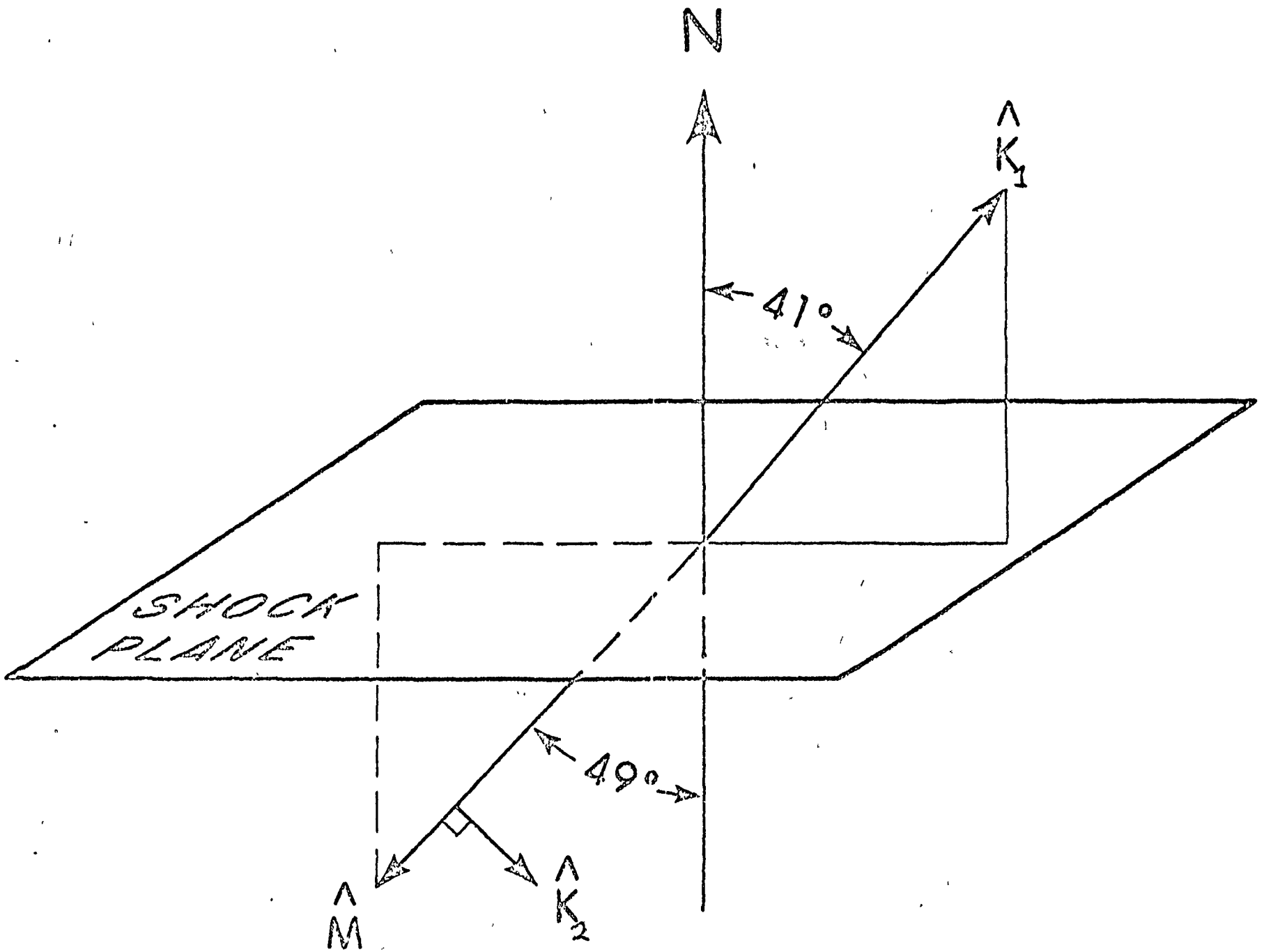
N
$\hat{K}_1$
41°
SHOCK
PLANE
49°
$\hat{M}$
$\hat{K}_2$